

20thth February 2020

RE: -Processing and Interpretation. – Magnetic Survey Data EL18/2018

1. Summary

Western Geophysics Pty Ltd (WGPX) has completed the processing, analysis, and interpretation of airborne magnetic survey data over exploration licence E18/2018.

The aim of the work is to investigate magnetic anomalies in a NW-SE trend within the Mathinna group sediments adjacent to the western margin of the Eddystone batholith and, to determine the depth and 3D structure of the magnetic sources.

Model calculations using 3D inversion and forward methods have shown the derived magnetic susceptibility values and depth of the source bodies are comparable and are 2 to 3 orders of magnitude higher than the weakly magnetic Mathinna group sediments.

The depth to the modelled bodies is relatively benign in terms of drilling targets and could be easily tested using RC drilling methods in most cases.

The work completed here forms a basis for target selection assuming the magnetic targets represent a part of the alteration and mineralisation process. Magnetic anomalies in the southern and Northern projects areas correlate with residual gravity anomalies (previous work) suggesting mass addition due to magnetite and pyrrhotite.

2. Introduction and Background

A regional magnetic and radiometric survey was flown by GPX Airborne Geophysics (200m line spacing) in 2005. The survey completely covers E18/2018

Previous work by WPX identified coincident magnetic and residual gravity anomalies trending NW-SE. The anomalies within the Mathinna group sediments are located at or near the contact of the Mathinna group with the Eddystone batholith. The magnetic and gravity anomalies are interpreted as being due to magnetite and/or pyrrhotite alteration in fault and fold structures within the Mathinna formation. (Figure 1)

Physical property work by Micheal Roach (Phd.1994) shows the granites have a relatively low density, averaging 2.61 T/m³ and are non-magnetic. Granodiorites have a mean density of 2.71 T/m³. The Mathinna Group rocks have a mean density of 2.71 T/m³. and are weakly magnetic (0.00019 SI units). Roach also correlates ground magnetic anomalies with increased magnetic susceptibility values in alteration associated with mineralised quartz veins in trenches near the Portland and Prince Imperial mines.

3. Geophysics Surveys and Data Processing.

Selected flight line covering EL18-2018 have been extracted from the database to enable further processing and modelling.

Gridding and imaging of the data show there is distinctive trend of magnetic anomalies and structure trend within a broad magnetic zone that is approximately 15km long (Figure 2). Peak magnetic anomaly amplitudes vary from approximately 50-110 nanoTesla (nT).

4. Magnetic Modelling and Interpretation.

Magnetic modelling has been completed using 3Dinversion software MGInv3D. (Scicomap Pty Ltd) and forward modelling software Model Vision (Pitney Bowes).

Flight line profiles have been selected across the maximum TMI anomalies (Figure 3). The key lines are described as being in the Southern, Central and Northern anomaly areas.

Trial and error forward modelling also incorporated the first vertical derivative (1Vd) of TMI which is sensitive to calculated depth. A good fit between the observed and calculated data has been achieved using simple tabular bodies. Apart from L101350 very deep sources greater than 500m BGL are simulated using the regional field.

Modelling using the 3Dinversion code has produced a 50m (X,Y) and 25m(Z) block model of calculated magnetic susceptibility values to a total depth of 1.8km. Depth slices through the model are shown as images on Figure 4. The 3D model calculation was completed using a multitasking 16 core (32 thread) high-end desktop computer. The starting model comprised 8 million cells. The forward and inverse modelling results presented as sections are shown together for each line on Figures 5 to 10. The location, depth to the top and the calculated magnetic susceptibility of the forward model bodies are posted below each of the sectional figures and, also on an image of TMI on Figure 11.

Calculated depth and magnetic susceptibility values are comparable for forward and inverse results. Magnetic susceptibility values from the 3D inversion however tend to be systematically lower by approximately 20% due to value spreading in the 50x 50m mesh.

5. Conclusions and Recommendations.

The aim of the work is to investigate magnetic anomalies in a NW-SE trend within the Mathinna group sediments adjacent to the western margin of the Eddystone batholith and, to determine the depth and 3D structure of the magnetic sources.

Model calculations using 3D inversion and forward methods has shown the derived magnetic susceptibility values and depth of the source bodies are comparable and are 2 to 3 orders of magnitude higher than the weakly magnetic Mathinna group sediments.

The depth to the modelled bodies is relatively benign in terms of drilling targets and could be easily tested using RC drilling methods in most cases.

The work completed here forms a basis for target selection assuming the magnetic targets represent a part of the alteration and mineralisation process. Magnetic anomalies in the southern and Northern projects areas correlate with residual gravity anomalies (previous work) suggesting mass addition due to magnetite and pyrrhotite.

Further geophysical methods that are most likely to assist in final target selection are ground magnetics, in-fill gravity and induced polarisation in selected areas.

FIGURES.

Figure 1. Northeast Tasmania Portland project tenements (red outlines) and mineral deposit locations.

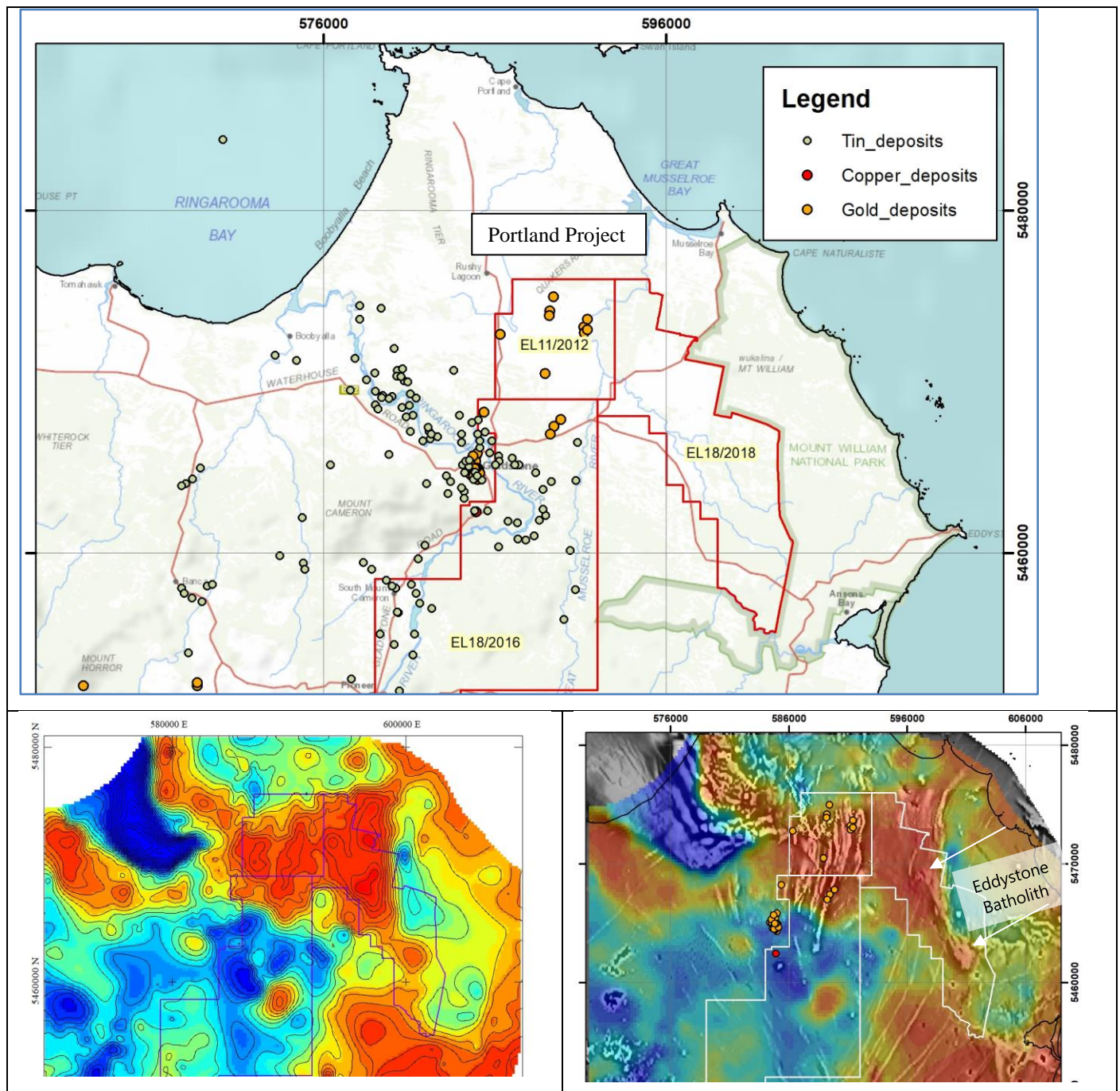


Figure 1. Exploration licence E18/2018 Northeast Tasmania with gold and tin occurrences(top). Residual gravity highs correlate with Mathinna Group sediments (bottom left) and gold occurrences correlate with magnetic anomalies. Distinctive magnetic anomalies (arrows) within the Mathinna group are located at or near to the Eddystone batholith contact as indicated on the map (lower right).

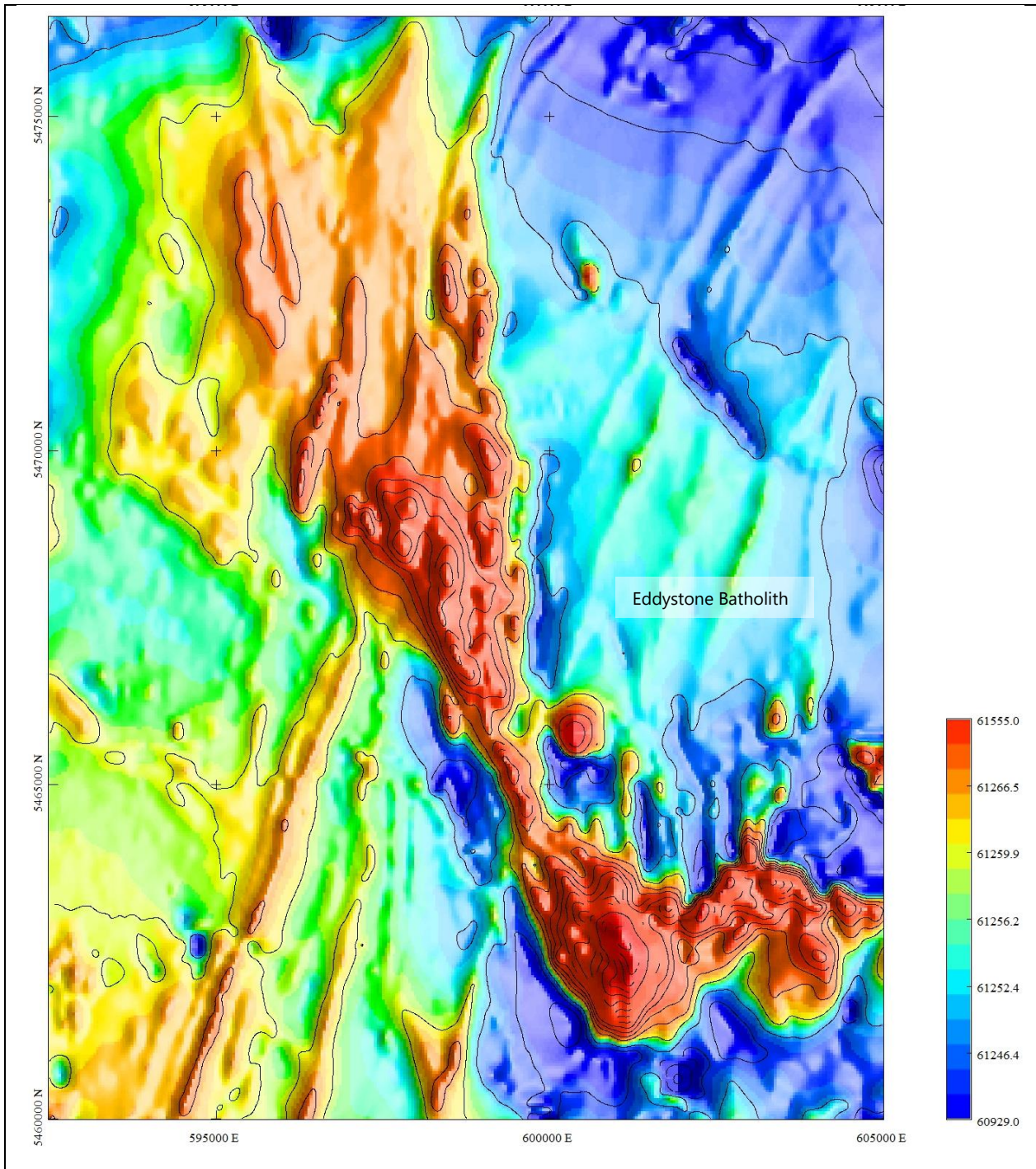


Figure 2. Imaged and contoured total magnetic intensity over E18/2018

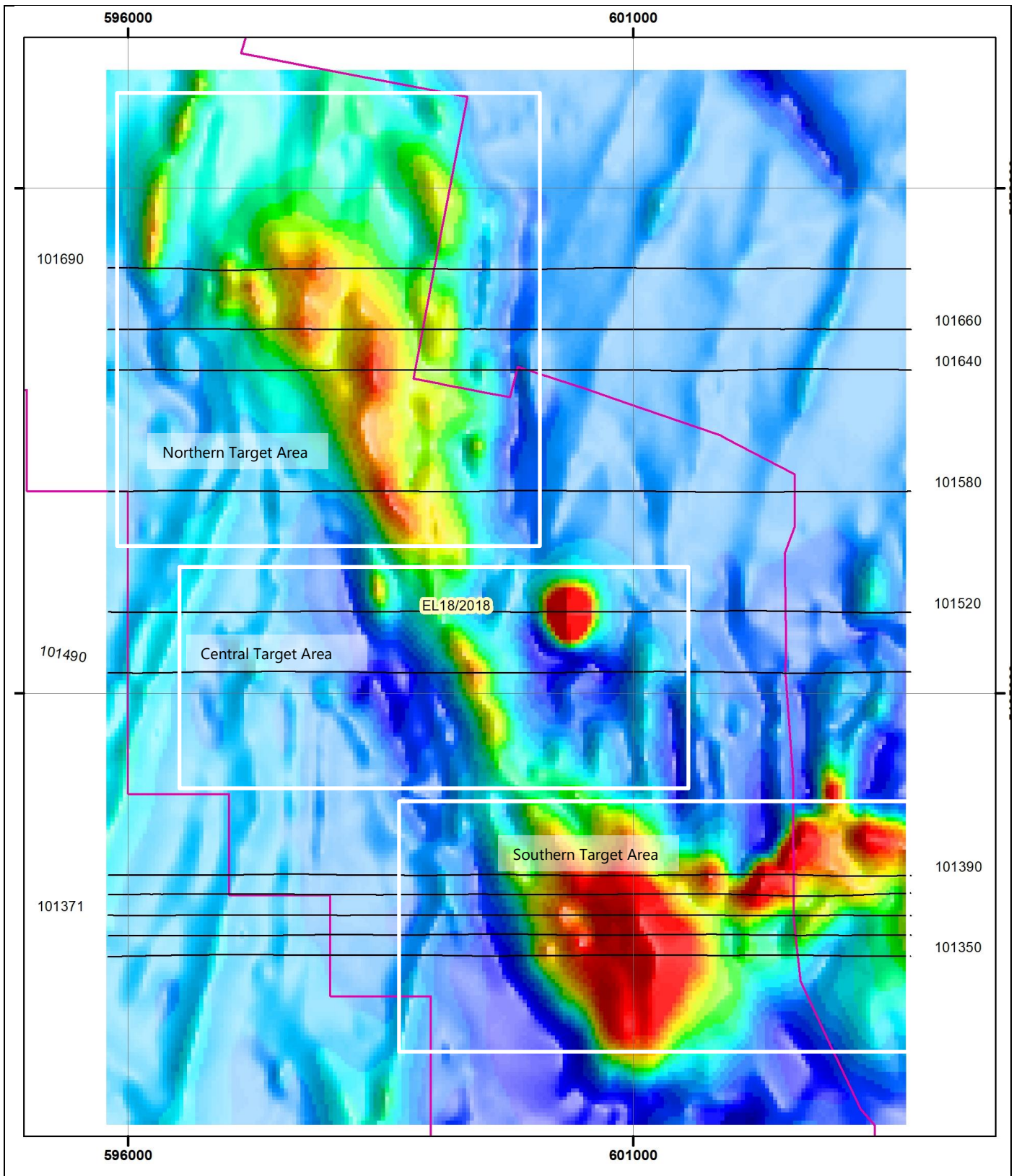


Figure 3. The total magnetic intensity (TMI) image over E18/2018. 3D model inversions were completed over the area of the TMI image. Forward model calculations were completed on selected flight lines, covering the Northern, Central and Southern magnetic target areas

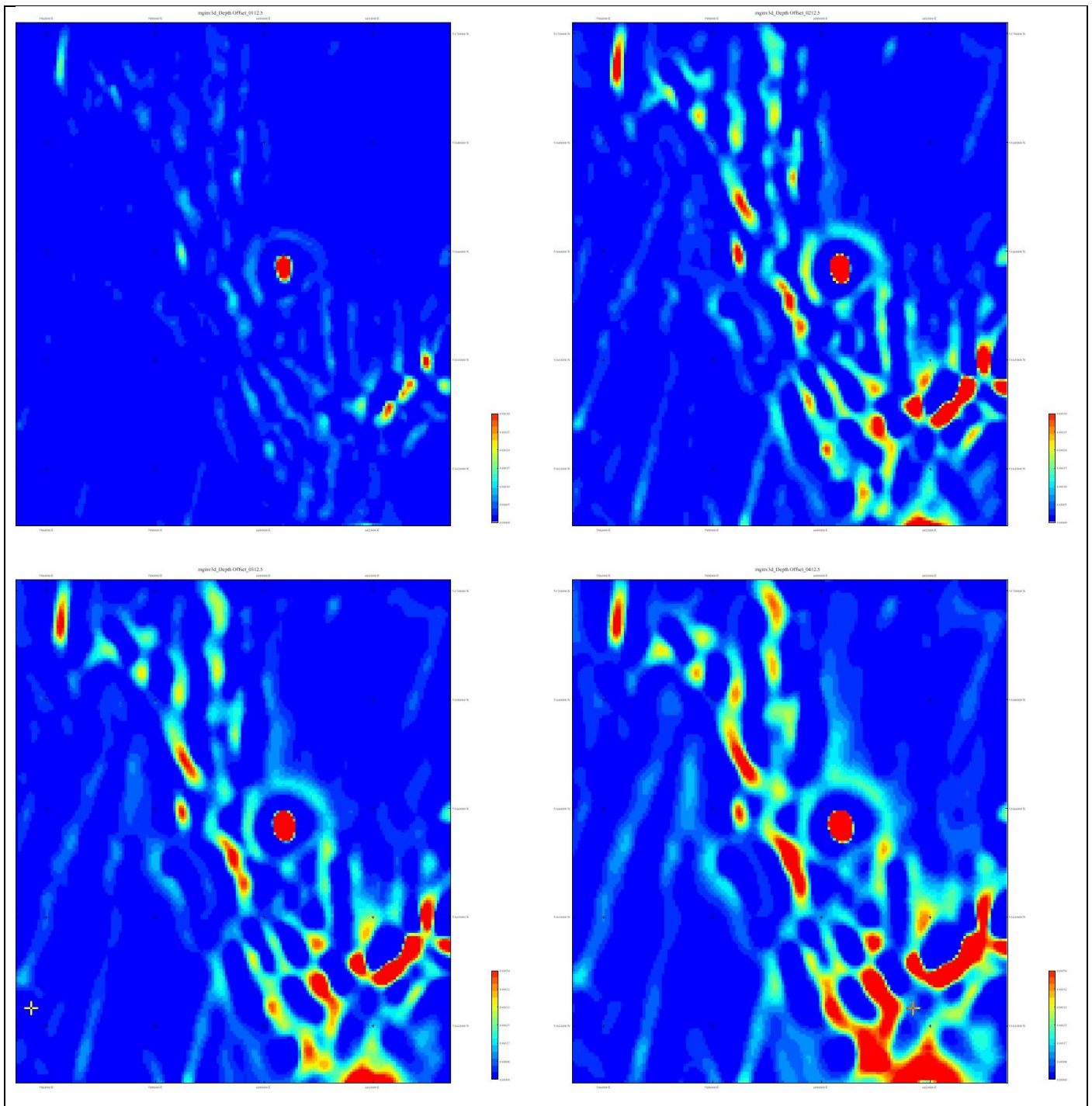


Figure 4. Depth slices through the 3D inversion model. At the top and left to right, depth slices are at 100m and 200m and at the bottom, 300m and 400m below the surface.

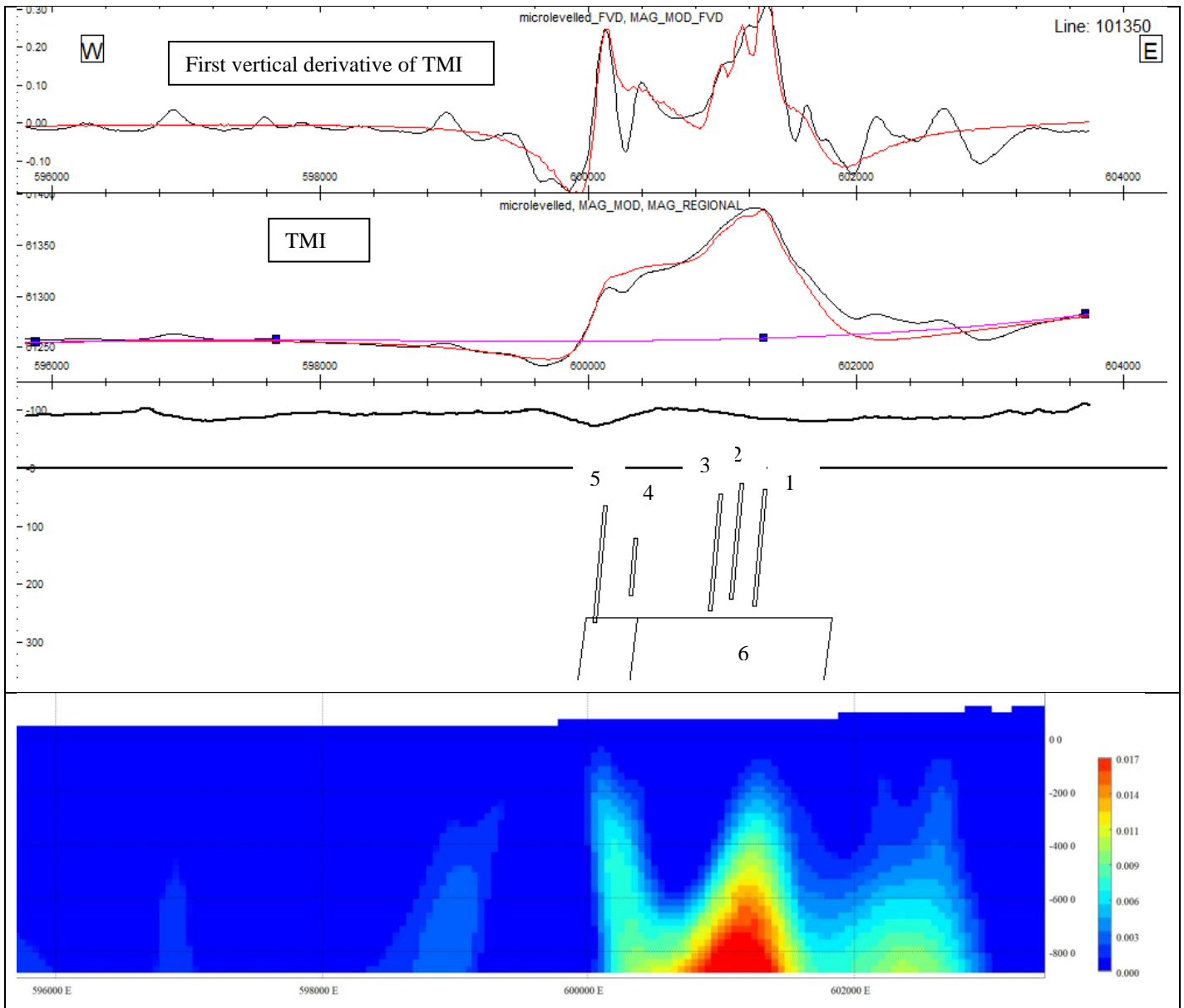


Figure 5. Southern target area magnetic modelling results. Forward modelling results line 101350 (top) and 3D inversion model section (bottom) Forward model properties are tabulated for each body. The forward and inverse model depth and magnetic susceptibility solutions are comparable. Vertical scales are RL in meters above or below mean sea level.

Line	BodyID	X	Y	Msus	DTM	Z	DepthBGL
101350	1	601321.1	5462400	0.03	73.85	-37.1	110.95
101350	2	601147.1	5462400	0.02	70.93	-25.1	96.03
101350	3	600990.5	5462400	0.02	69.06	-45.2	114.26
101350	4	600355.4	5462400	0.01	71.9	-119.7	191.6
101350	5	600129.2	5462400	0.03	75.36	-65.3	140.66
101350	6	600903.5	5462400	0.02	70.32	-258	328.32

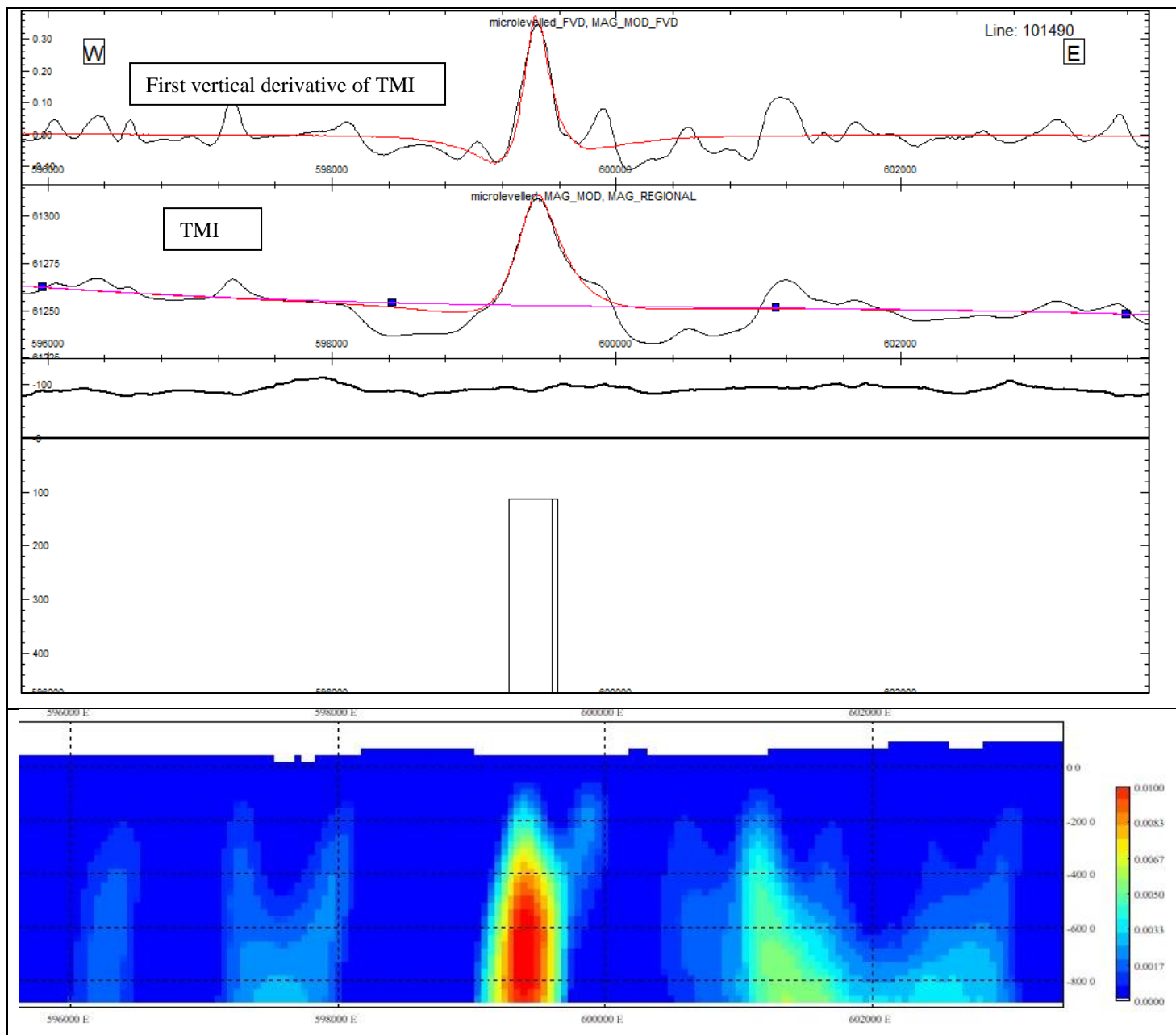


Figure 6. Central target area magnetic modelling results. Forward modelling results line 101490 (top) and 3D inversion model section (bottom) Forward model properties are tabulated for each body. The forward and inverse model depth and magnetic susceptibility solutions are comparable. Vertical scales are RL in meters above or below mean sea level.

Line	BodyID	X	Y	Msus	DTM	Z	DepthBGL
101490	1	599417.3	5465205	0.05	50.27	-112.1	162.37

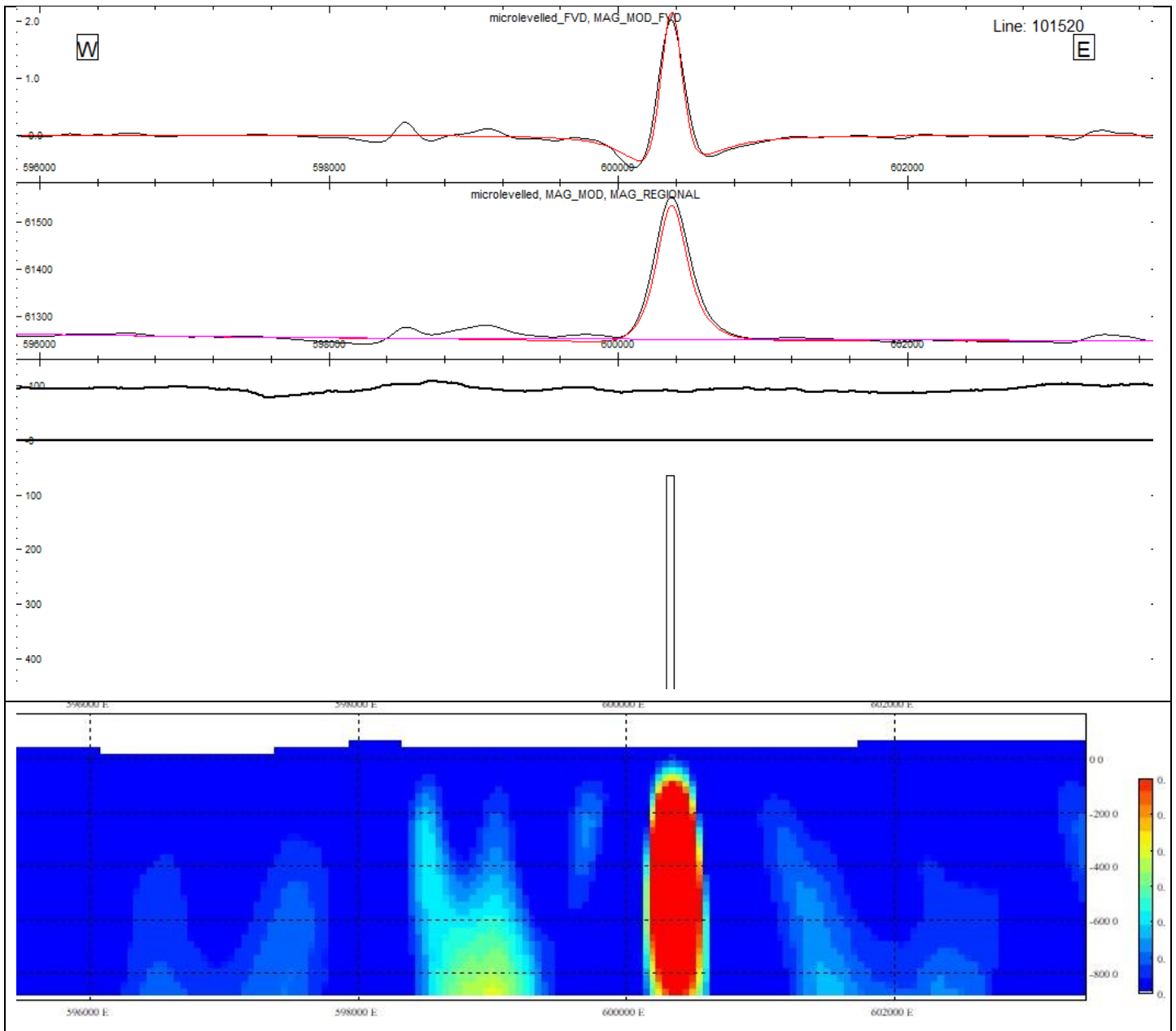


Figure 7. Central target area magnetic modelling results. Forward modelling results line 101520 (top) and 3D inversion model section (bottom) Forward model properties are tabulated for each body. The forward and inverse model depth and magnetic susceptibility solutions are comparable. Vertical scales are RL in meters above or below mean sea level.

Line	BodyID	X	Y	Msus	DTM	Z	DepthBGL
101520	1	600359.3	5465800	0.17	49.41	-55.75	105.16

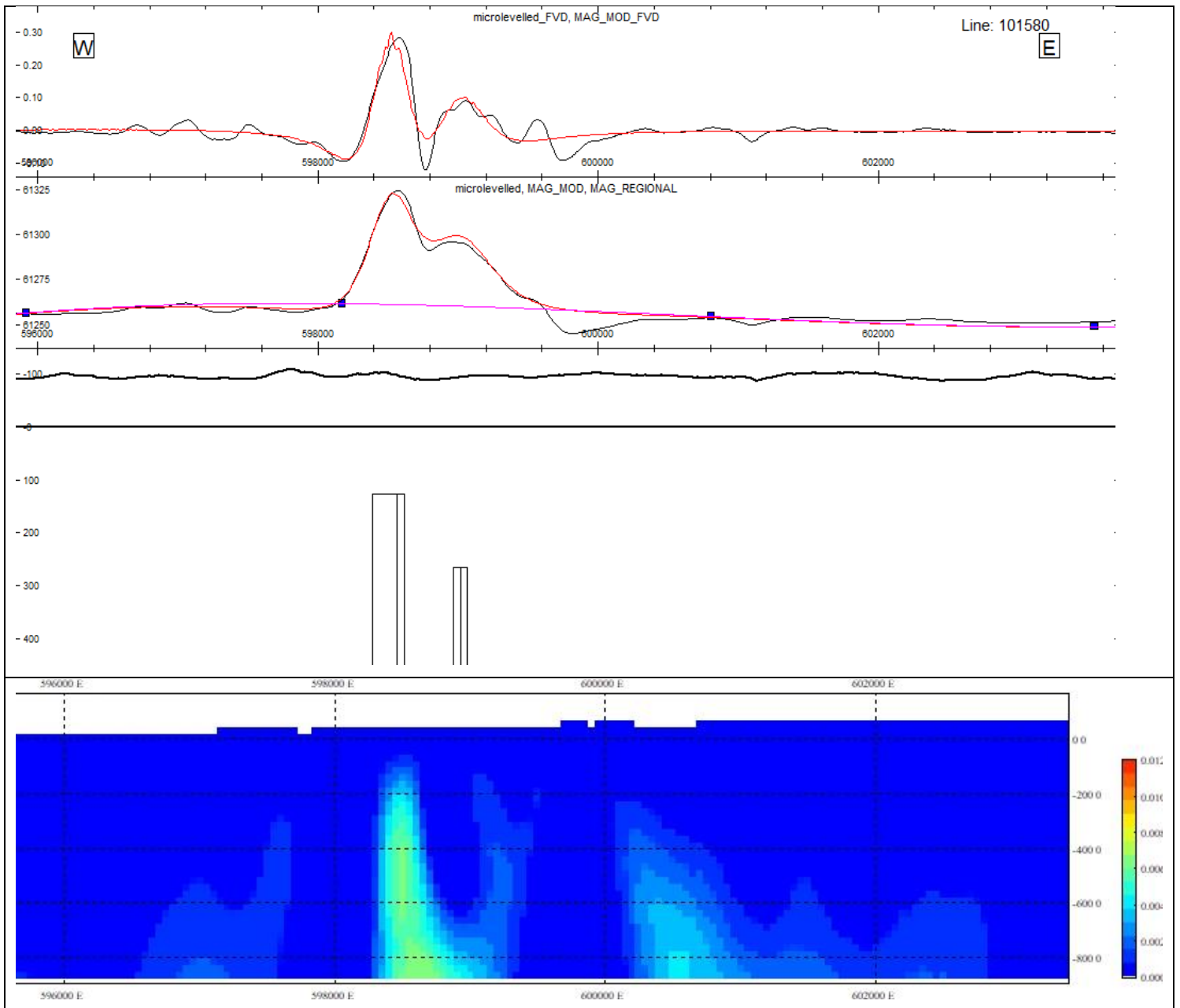


Figure 8. Northern target area magnetic modelling results. Forward modelling results line 101580 (top) and 3D inversion model section (bottom) Forward model properties are tabulated for each body. The forward and inverse model depth and magnetic susceptibility solutions are comparable. Vertical scales are RL in meters above or below mean sea level.

Line	BodyID	X	Y	Msus	DTM	Z	DepthBGL
101580	1	598504.4	5467000	0.04	36.61	-126.29	162.9
101580	2	599016	5467000	0.07	45.44	-266.52	311.96

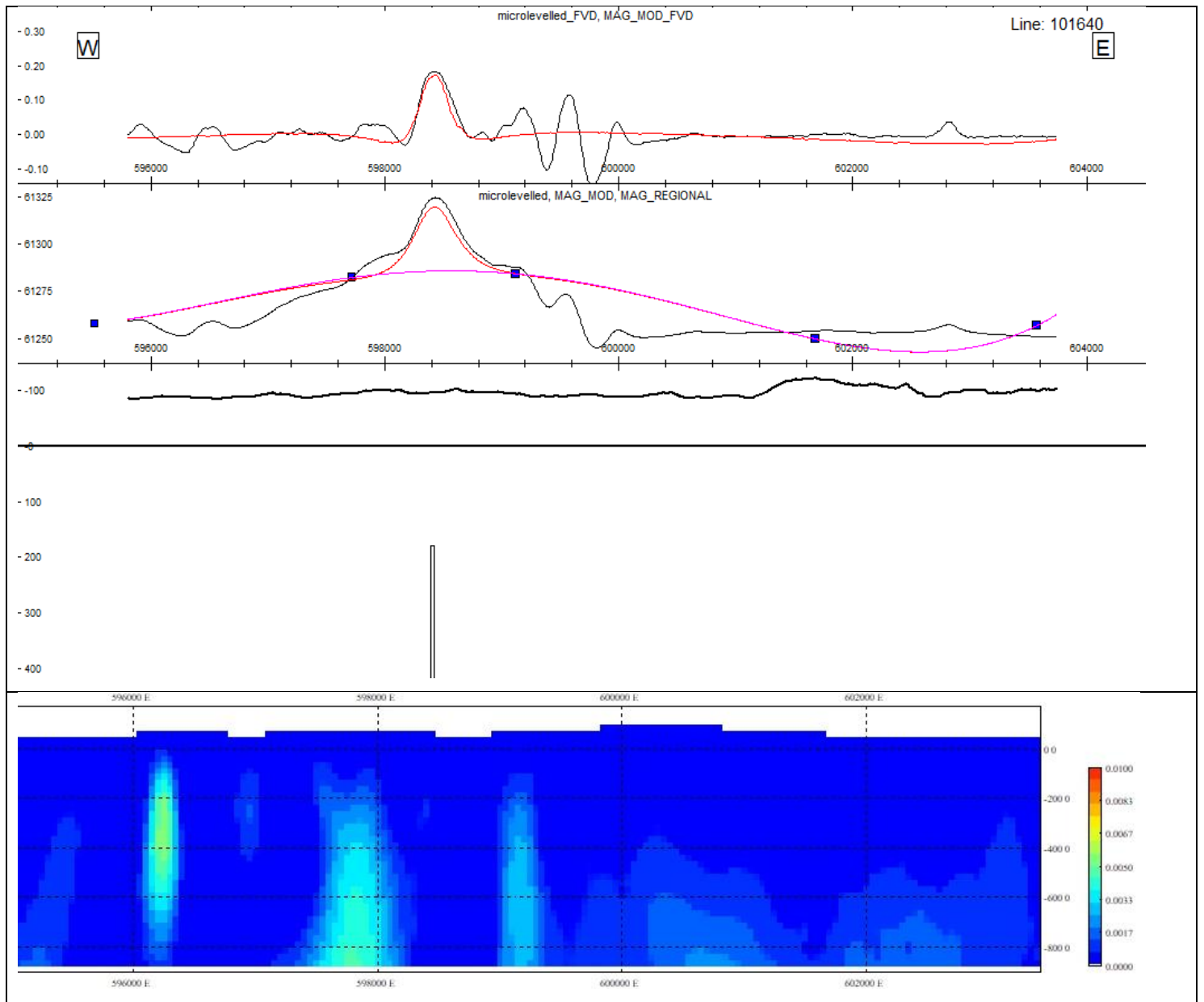


Figure 9. Northern target area magnetic modelling results. Forward modelling results line 101640 (top) and 3D inversion model section (bottom) Forward model properties are tabulated for each body. The forward and inverse model depth and magnetic susceptibility solutions are comparable. Vertical scales are RL in meters above or below mean sea level.

Line	BodyID	X	Y	Msus	DTM	Z	DepthBGL
101640	1	598408.2	5468167	0.06	44.77	-180	224.77

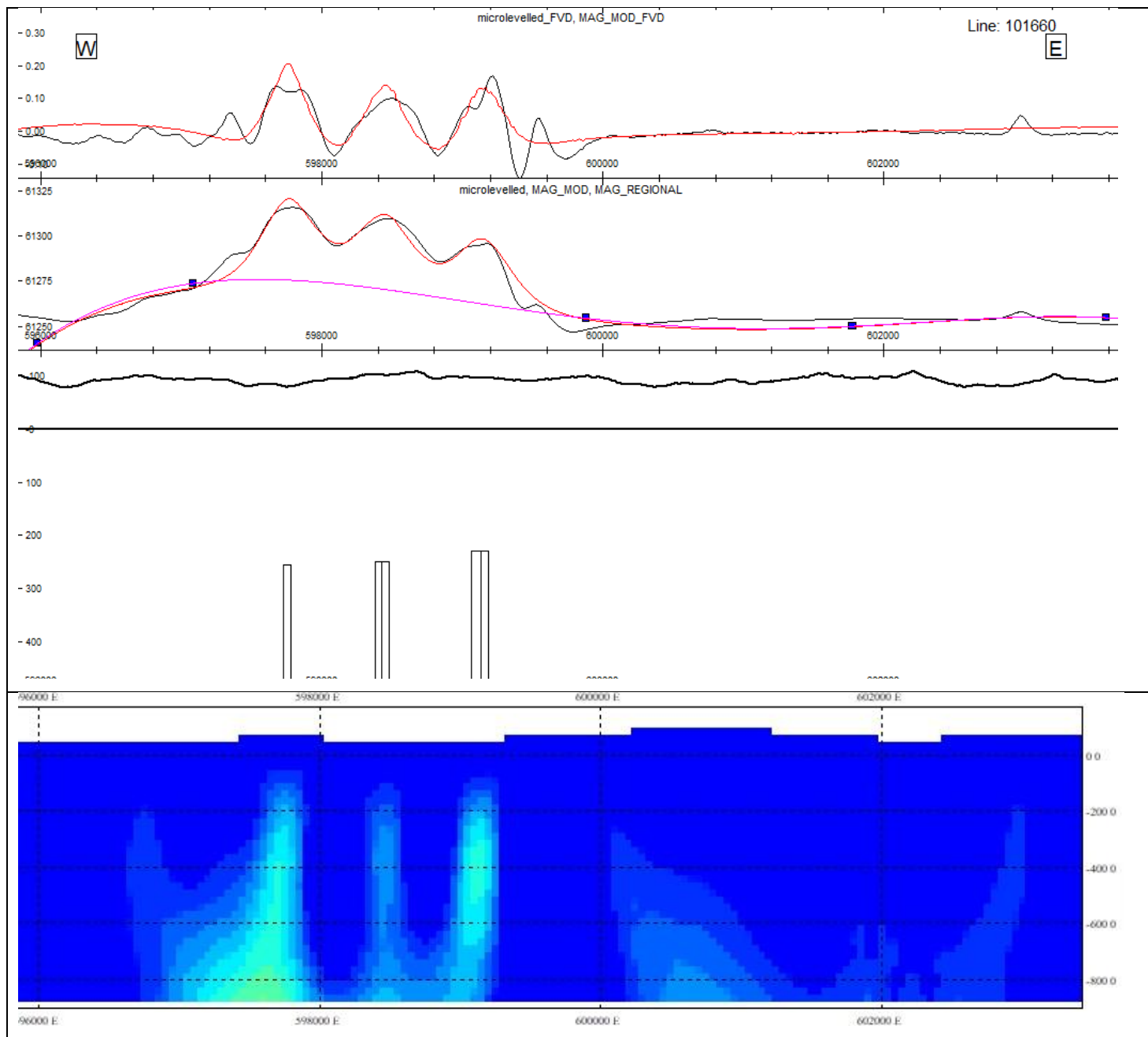


Figure 10. Northern target area magnetic modelling results. Forward modelling results line 101660 (top) and 3D inversion model section (bottom) Forward model properties are tabulated for each body. The forward and inverse model depth and magnetic susceptibility solutions are comparable. Vertical scales are RL in meters above or below mean sea level.

Line	BodyID	X	Y	Msus	DTM	Z	DepthBGL
101660	1	597752.3	5468574	0.08	61.66	-256.5	318.16
101660	2	598429.6	5468609	0.08	50.33	-250.4	300.73
101660	3	599123.5	5468609	0.06	50	-230.3	280.3

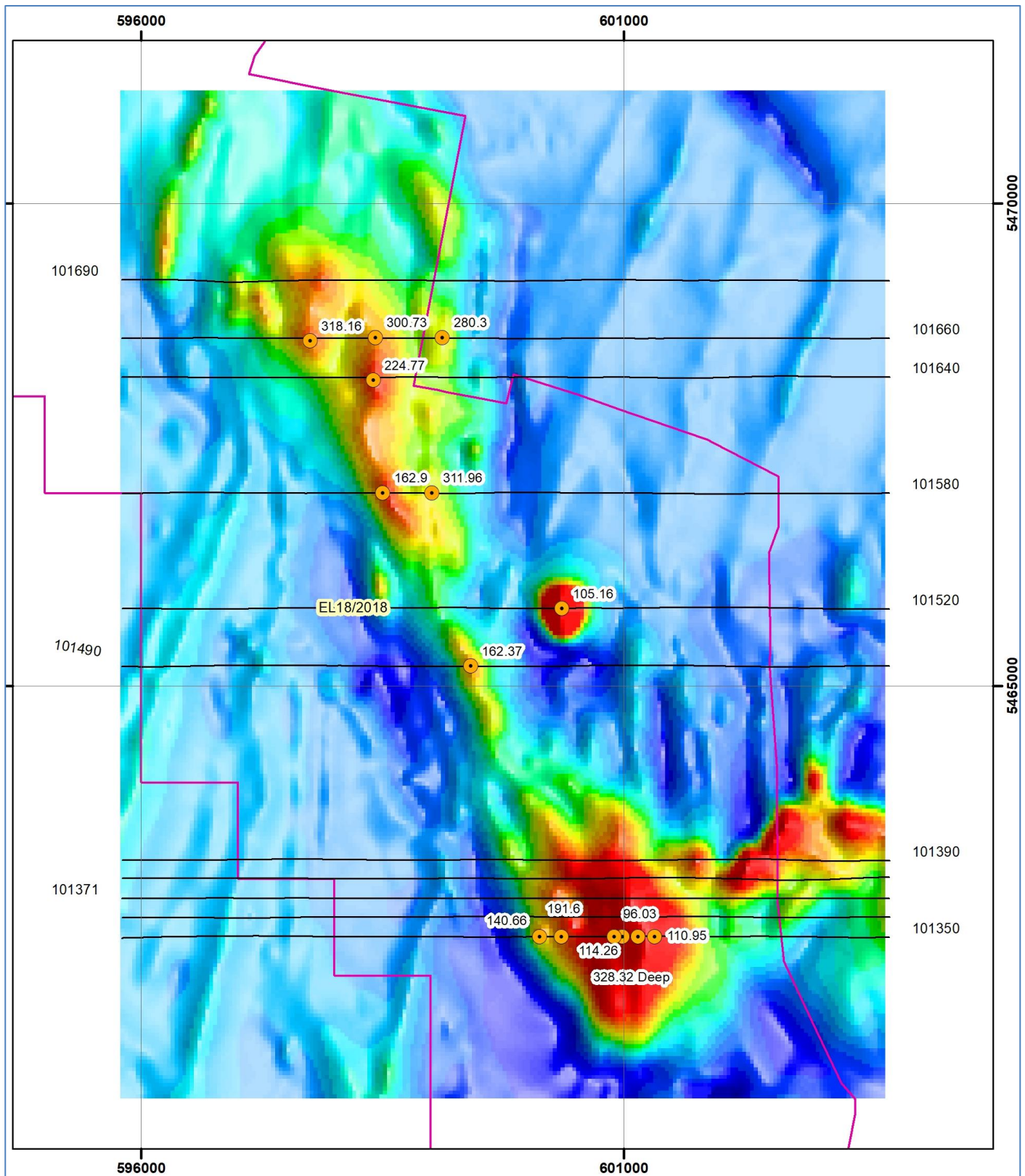


Figure 10. Forward modelling, calculated top of magnetic bodies on selected lines. The background image is TMI.